

172 201-1957

EA-6010-19  
Dist. Category UC-90C

MATERIALS RESEARCH FOR THE CLEAN UTILIZATION OF COAL

QUARTERLY PROGRESS REPORT

January - March 1979

Samuel J. Schneider  
Project Manager

Center for Materials Science  
National Bureau of Standards  
Washington, D. C. 20234

PREPARED FOR THE UNITED STATES  
DEPARTMENT OF ENERGY

Under Contract No. EA-77-A-01-6010

This report was prepared as an account of work sponsored by the United States Government. Neither the United States nor the United States Department of Energy, nor any of their employees, nor any of their contractors, subcontractors, or their employees, makes any warranty, express or implied, or assumes any legal liability or responsibility for the accuracy, completeness, or usefulness of any information, apparatus, product or process disclosed, or represents that its use would not infringe privately owned rights."



TABLE OF CONTENTS

	PAGE
I. OBJECTIVE AND SCOPE OF WORK. . . . .	1
II. SUMMARY OF PROGRESS TO DATE. . . . .	1
Articles Published and Talks Presented . . . . .	3
III. DETAILED DESCRIPTION OF TECHNICAL PROGRESS . . . . .	5
1. Metal Corrosion. . . . .	5
a. Pre-Cracked Fracture Test. . . . .	5
2. Ceramic Deformation, Fracture and Erosion. . . . .	9
3. Chemical Degradation . . . . .	12
a. Reactions and Transformations. . . . .	12
b. Slag Characterization. . . . .	13
c. Vaporization and Chemical Transport. . . . .	14
4. Failure Prevention . . . . .	26
a. Failure Information Center . . . . .	26
b. Materials Properties Data Center . . . . .	30



## I. OBJECTIVE AND SCOPE OF WORK

Coal Gasification processes require the handling and containment of corrosive gases and liquids at high temperature and pressures, and also the handling of flowing coal particles in this environment. These severe environments cause materials failures which inhibit successful and long-time operation of the gasification systems. The project entails investigations on the wear, corrosion, chemical degradation, fracture, and deformation processes which lead to the breakdown of metals and ceramics currently being utilized in pilot plants. Studies will also be carried out on new candidate materials considered for improved performance. Special emphasis will be devoted to the development of test methods, especially short-time procedures, to evaluate the durability of materials in the gasification environments. These methods will focus on wear, impact erosion, stress corrosion, strength, deformation, slow crack growth and chemical degradation. A system has been initiated to abstract and compile all significant operating incidents from coal conversion plants as well as materials property and performance information important to the design and operation of these plants. This program will provide a central information center where problems of common interest can be identified and analyzed to avoid unnecessary failures and lead to the selection of improved materials for coal conversion and utilization. Active consultation to DOE and associated contractors will be provided as requested.

## II. SUMMARY OF PROGRESS TO DATE

### Brief Summary

#### 1. Metal Corrosion

##### a. Pre-cracked Fracture Test

Tests to experimentally verify the thermal-elastic stress analysis for the tension-loaded double-cantilever beam specimen were continued and modifications were made to the stress analysis to more accurately predict the change in stress-intensity with temperature. Tests to experimentally verify the stress analysis were conducted using specimens of both A.I.S.I. type 304 and type 310 stainless steel. The test fixture for loading double cantilever beam specimens was modified to permit testing to higher stress-intensity levels and to permit testing a wider range of specimen materials.

#### 2. Ceramic Deformation, Fracture and Erosion

Efforts this quarter culminated with the completion of the first successful experiment in the apparatus for mechanical testing at elevated pressure and temperature. A second experiment was in progress at the end of the quarter. Problems encountered with the apparatus last quarter and at the beginning of this quarter were corrected to establish the operation of the system. These modifications to the apparatus and results from the experiment are described in the text.

Depending upon the successful completion of the experiment currently in progress, controlled experimental studies will begin on newly prepared batches of both high and low-alumina refractory concretes with steam as the reactive exposure environment. Initial temperatures of consideration will be 310°C, 610°C, and 1010°C. If possible, additional specimens will be exposed with the specimens for the *in situ* testing, so that strength-after-exposure can be correlated with the strength determined at pressure and temperature.

### 3. Chemical Degradation

#### a. Reactions and Transformations

In the dry gas (42% H<sub>2</sub>, 33% CO, 25% CO<sub>2</sub>) environment,  $\bar{C}\bar{C}$  (CaCO<sub>3</sub>) appears to be stable at 900 C and 540 psig. It dissociates at a much lower temperature when steam is present.

Preliminary *in situ* x-ray studies indicate that  $\bar{C}\bar{C}$  is stable in an atmosphere of CO<sub>2</sub> at 1100°C and 500 psig.

#### b. Slag Characterization

A synthetic slag high in alkali composition (20 wt %) tended to exhibit viscosity values higher in steam pressure than those recorded at ambient pressure. This effect was probably due to polymerization in the melt. When the alkali content was reduced to five weight percent the viscosity was reduced in the presence of steam. The viscosity of a slag with the following composition expressed in wt %, SiO<sub>2</sub>, 48.30%; Al<sub>2</sub>O<sub>3</sub>, 12.10%; Fe<sub>2</sub>O<sub>3</sub>, 12.00%; CaO, 14.90%; MgO, 8.00% and Na<sub>2</sub>O, 4.7% was measured in 80 psi steam. The viscosity values were determined at 1275, 1296, 1351, and 1370°C. The average values at these temperatures are log  $\eta$  = 1.88, 1.76, 1.56 and 1.44. The viscosity of this material appears to be lowered with increasing steam pressure. In addition the value of log  $\eta$  = 1.44 at 1370°C at both ambient pressure in air and 80 psi steam would indicate that the two viscosity curves tend to coalesce with increasing temperature. The viscosity of this slag was decreased significantly in the presence of 25 psi nitrogen, from 1.84 (in air) to log  $\eta$  = 1.71 (nitrogen) at 1279°C.

In addition to the effects on viscosity it should be noted that all of the environmental gases studied effect the crystallization of the slag at temperatures lower than 1300°C. This crystallization could have serious consequences in the Bi-gas process where the slag must remain fluid for removal at temperatures below 1300°C. It would appear that some slag modification experiments should be conducted to determine retardants for crystallization.

#### c. Vaporization and Chemical Transport

An extensive study has been made of vapor transport over a high melting temperature (~1700K) potassium-enriched slag derived from Illinois number 6 coal. The initial slag composition, in wt%, was: Al<sub>2</sub>O<sub>3</sub> (12.06), CaO (3.8), Cr<sub>2</sub>O<sub>3</sub> (1.3), Fe<sub>2</sub>O<sub>3</sub> (14.25), K<sub>2</sub>O (19.54), MgO (1.03), Na<sub>2</sub>O (0.47), SO<sub>3</sub> (0.21), SiO<sub>2</sub> (46.82), TiO<sub>2</sub> (0.52). For identification

purposes we shall denote this slag as  $K_1$ . X-ray diffraction data indicated that the bulk of the slag-K is present as the compound  $KAlSiO_4$ . About 2% of the K was present in relatively volatile form, mainly  $K_2SO_4$  and  $K_2CO_3$ . The rate of release of K, and secondary species such as  $H_2O$ ,  $O_2$ ,  $SO_2$ ,  $CO_2$  and Na, has been measured over the temperature range 1100-1820K, a  $N_2$ -pressure range of 0.2-0.63 atm, and for  $K_2O$  slag contents over the range 15.4-8.0 mole %. Apparent activity coefficients for  $K_2O$  in the range of  $10^{-9}$  -  $10^{-7}$  were determined for this regime of temperature and composition. Evidence for diffusion-limited alkali transport in the bulk slag was obtained and the observed partial pressures and activity coefficients may be a factor of 2-10 lower than the true thermodynamic equilibrium values.

We plan to extend this study to include the effects of variable applied  $H_2O$  pressure and of chloride additions on the release of K from the  $K_1$  slag system. Similar studies will also be initiated on a relatively low melting ( $\approx 1500K$ ) synthetic slag of composition wt%,  $SiO_2$  (47.3),  $Al_2O_3$  (11.1),  $Fe_2O_3$  (12),  $CaO$  (13.9),  $MgO$  (7.0), and  $K_2O$  (8.7). Complementary mathematical modeling of alkali vaporization from these slags, and their equilibrium reactions with coal gas constituents, will also be initiated.

#### 4. Failure Prevention

##### a. Failure Information Center

Eight additional reports of operating experiences and failure analysis were entered into the Center's data base. Over 380 information items were transmitted to plant operators and fossil energy contractors. The final draft of the report covering the performance of materials and components at the  $CO_2$  Acceptor Pilot Plant was completed and additional progress was made in completing detailed analysis of reported corrosion and erosion failures. The Center's data base is being revised in format and content to aid in future information dissemination and a joint project with the Materials Properties Data Center has been started.

##### b. Materials Properties Data Center

During this quarter an outline for a data Handbook for construction materials for coal gasification has been prepared, submitted to DOE, and been approved by the project monitor. Sections of the Handbook are being prepared. Data both on coal conversion materials of construction and MHD materials are being prepared for entry into a computer system although a computer vendor's services have not yet been procured.

#### Articles Published and Talks Presented

"Erosion of Ceramics", S. M. Wiederhorn, Conference on Erosion/Corrosion of Coal Conversion System Materials held at Lawrence Berkeley Laboratories, Berkeley, CA., January 24-26, 1979.

"Mechanisms of Erosive Wear in Ceramic Materials", S. M. Wiederhorn, Cornell University, Ithaca, New York, April 4-5, 1979.

"Erosion of Ceramics", S. M. Wiederhorn, Proceedings of NACE Conference on Erosion/Corrosion of Coal Conversion System Materials held at Lawrence Berkeley Laboratories, Berkeley, CA., January 24-26, 1979.

F. A. Mauer and C. R. Robbins, "X-ray Powder Diffraction Measurements in Reactive Atmospheres at 1000 °C and 7 MPa (1000 psig)," to be published in Advances in X-ray Analysis, vol. 22 (1979).

"Materials Performance in Advance Coal Conversion Pilot Plants", R. C. Dobbyn, invited talk, Oak Ridge National Laboratory, March 1, 1979, Oak Ridge, TN.



### III. DETAILED DESCRIPTION OF TECHNICAL PROGRESS

#### 1. Metal Corrosion

##### a. Pre-cracked Fracture Test (J. H. Smith and G. E. Hicho, 562)

Progress: Tests were conducted to experimentally verify the analysis for the change in stress-intensity ( $K_T/K_0$ ) with temperature given in reference 1. These tests consisted of measuring the change in displacement at the crack line ( $V_t$ ) in the double-cantilever beam (DCB) specimen as a function of temperature. The stress analysis shows that the change in stress-intensity with temperature ( $K_T/K_0$ ) is a function of the change in crack line displacement with temperature ( $V_t/V_0$ ) and the change in elastic modulus of the specimen with temperature ( $E_t/E_0$ ) as given by the following equation:

$$\frac{K_t}{K_0} = \left(\frac{E_t}{E_0}\right) \left(\frac{V_t}{V_0}\right)$$

The terms  $K_0$ ,  $E_0$ ,  $V_0$  represent the value of the stress-intensity, elastic modulus, and crack line displacement at the reference temperature ( $0^\circ\text{C}$ ). Reliable values of the change in elastic modulus of the test specimen with temperature ( $E_t/E_0$ ) are obtained from published data on the properties of metals.

Double-cantilever beam specimens of A.I.S.I. type 304 stainless steel were tested in a loading fixture made of 304 stainless steel with a loading grip made from Inconel 600. Several test runs were made in which the crack line displacement,  $V_t$ , was measured with a measuring microscope as shown in Figure 1. Test runs were made to measure  $V_t$  as a function of temperature up to  $600^\circ\text{C}$ .

These test runs demonstrated that the test specimen expanded with increased temperature in a manner which should allow the applied stress-intensity,  $K_T$ , to remain constant with increasing temperature as predicted by the stress analysis. The results of the series of tests were reasonably reproducible from test to test. However, the accuracy of the measurement of the crack line displacement,  $V_t$ , must be improved to reliably verify the theoretical stress analysis.

The loading fixture for stressing the tension-loaded double-cantilever beam specimen was redesigned to permit testing of specimens to higher values of stress-intensity and to permit testing a wider range of specimens. This new design test fixture is shown in Figure 2. The new test fixture was fabricated from a stabilized grade of stainless steel (type 347) and the grips were made of Inconel 600. A specimen of type 310 was loaded to stress-intensity levels up to 25 Ksi in. Several test runs were made in which a test specimen was heated to  $600^\circ\text{C}$  and the crack line displacement,  $V_t$ , was measured as a function of temperature. Reproducible test results were obtained but more precise measurements will be required to verify the predicted change in stress-intensity level with temperature.

Specimens were prepared for testing in aggressive environments at elevated temperatures. Specimens of type 304, 310 stainless steel, and Incoloy 800 have been obtained and fatigue cracked in preparation for testing. The threshold stress-intensity ( $K_{Isc}$ ) will be determined as a function of temperature for these specimens in an  $H_2S$ -steam environment.

Plans: The test fixture will be modified so that continuous measurements of the crack line displacement,  $v_t$ , as a function of temperature can be made. This will significantly improve the accuracy of these measurements.

The theoretical stress-analysis will be accurately verified for several combinations of specimens and grips and the sensitivity of the change in stress-intensity with temperature will be determined.

#### Reference

1. Quarterly Report, Jan. 1 - Mar. 31, 1978 "Materials Research for Clean Utilization of Coal," page 14.

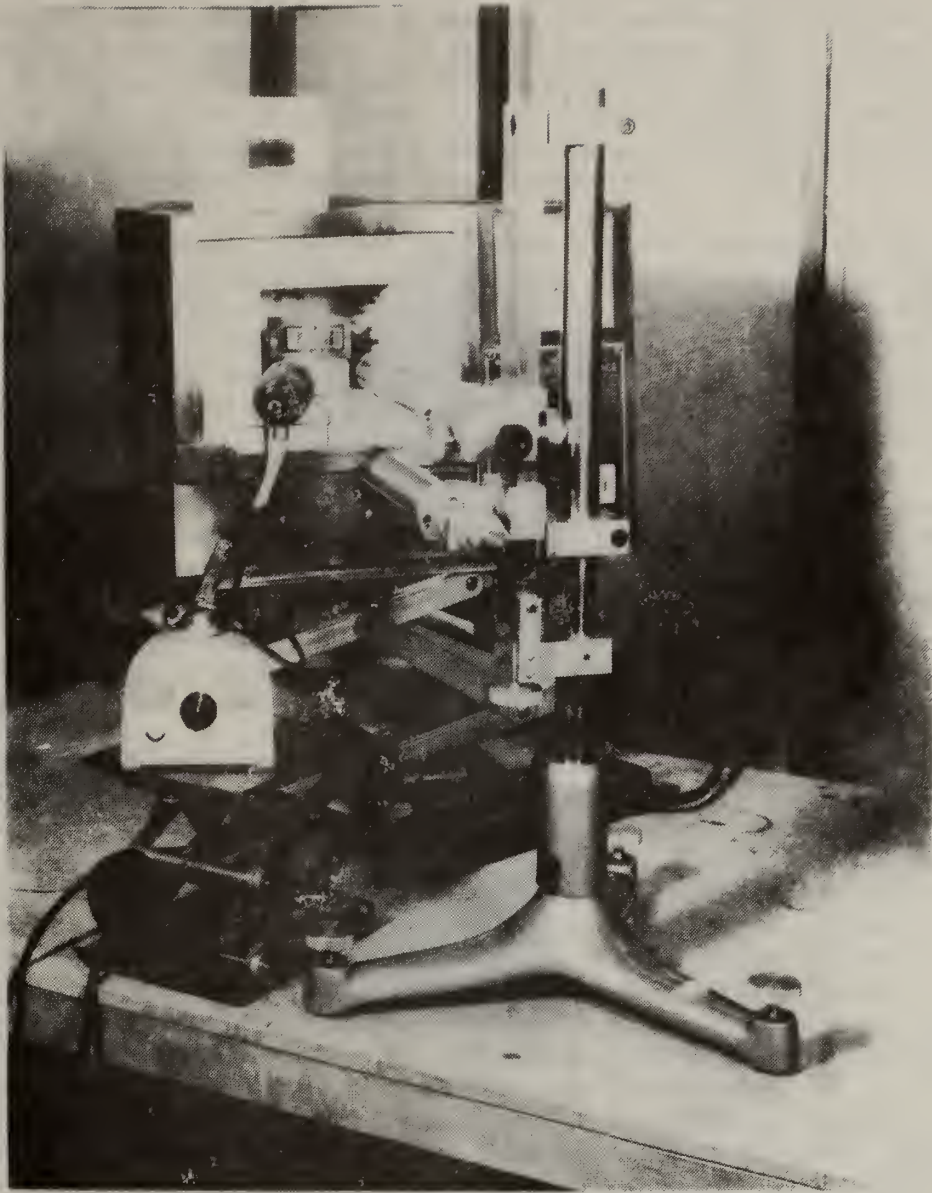


Figure 1. Test Set-up for Experimental Verification of Specimen Stress Analysis.



Figure 2. New Design of DCB Fixture.

2. Ceramic Deformation, Fracture, and Erosion (E. R. Fuller, Jr., S. M. Wiederhorn, D. E. Roberts, and Leon Chuck, 562.00)

Progress: Efforts this quarter culminated with the completion of the first successful experiment in the apparatus for mechanical testing at elevated pressure and temperature. A second experiment was in progress at the end of the quarter. Problems encountered with the apparatus last quarter and at the beginning of this quarter were corrected to establish the operation of the system. These modifications to the apparatus and the results from the experiment are described below.

While establishing the operation of the apparatus for mechanical testing in elevated pressure/temperature environments, initial experiments were conducted in a gaseous environment of CO<sub>2</sub> and N<sub>2</sub> at approximately 800°C and at a pressure of 69 MPa (1000 psia). Previously encountered difficulties with high pressure gas leakage into the hydraulic loading system appeared to have been corrected by an interim solution. This solution involved covering the sealing ring of the hydraulic piston with hydraulic oil, so that this oil would be forced into the hydraulic system before the pressurizing gas. A redesign of the sealing arrangement has also been considered. In this redesign another sealing ring would be installed around the loading piston in the reverse sense. An additional sealing ring has been received for this purpose, but since the interim solution appears to be working satisfactorily, modifications to the sealing arrangement will not be undertaken until they are necessitated by a reoccurring problem.

Another reoccurring problem has been over-heating of the load cell. To correct this problem a copper cooling jacket was designed to enclose the load cell. Unfortunately, this cooling jacket did not supply adequate cooling to the load cell as the temperature reached 114°C in a subsequent test run. Accordingly, the cooling jacket was redesigned so that it makes intimate contact with the load cell. In addition, the insulation in the upper region of the outer pressure vessel was increased and modified to reduce the temperature in the region of the load cell. Although these modifications have significantly reduced the temperature of the load cell, the temperature in subsequent experiments still reached 55°C. Accordingly, a technique was devised for calibrating the load cell at temperature and pressure. The technique utilizes a small differential pressure between the inner and outer pressure vessel to apply a load to the load cell. The effective area of the bellows, necessary to calculate this force, was determined from a similar room temperature calibration against dead weights.

In the experiment for which the load cell temperature reached 114°C, specimens of a low-alumina refractory concrete were broken in three-point flexural loading in a CO<sub>2</sub> environment at 800°C and 700 psia pressure. Although the breaking load readings are in error due to the temperature shift of the load cell calibration, that was not determined at that time, the measured strengths of approximately 10 MPa are slightly higher than the strengths of control specimens that were not exposed.

Having increased the insulation in the upper region of the outer pressure vessel and having redesigned the load cell cooling jacket, another experiment was begun on the low-alumina refractory concrete in an environment of N<sub>2</sub> and steam. The initial pressure/temperature conditions were 1.28 MPa (185 psia) and 300°C. After a 24 hour exposure, the longest to date in this apparatus, the temperature was raised to 800°C with the pressure increasing to 2.96 MPa (430 psia). The revised cooling jacket and extra insulation worked satisfactorily with the temperature of the load cell reaching only 43°C. The experiment was terminated, however, because of a leak that developed in the gasket seal between the inner and outer vessels. This leak was detected by the loss of steam pressure from the inner vessel, and appeared to have resulted from overheating of the copper gasket that sealed the end flange. To rectify this problem, nickel gaskets are being prepared to replace the present copper gaskets. In addition, the temperature profile around the upper flange was reduced somewhat by modifications to the insulation of this region - mainly the packing density.

Since the system was working satisfactorily in all other regards, lower temperature experiments (up to 600°C) could be conducted while the nickel gaskets were being fabricated. The first of these experiments was conducted on a low-alumina refractory concrete in a steam environment. The exposure chamber (inner pressure vessel) was initially evacuated with a vacuum roughing pump and a controlled amount of water (150 ml.) was metered into the chamber. The system was then heated to 400°C to produce a steam environment of 2.07 MPa (300 psia). Following a 17 hour exposure at 400°C with a 2.07 MPa steam pressure, the specimen temperature was increased to 620°C with the steam pressure rising to 4.14 MPa (600 psia). The specimens were then exposed at this temperature and pressure for 100 hours before they were broken *in situ*. The median strength and the standard deviation from the four specimens tested are given in the Table below. Also tabulated are the median strength of two control specimens and the crystalline mineral phases in each type of specimen as determined by x-ray diffraction analysis. The phases listed for the exposed refractory specimens were determined on the specimens after cooling from pressure and temperature.

Median Strength and Standard Deviation for a Low-Alumina Refractory Concrete. The Strengths were measured at temperature and pressure with the mineral phases being determined subsequent to cooling.

<u>Exposure</u>	<u>In-situ Strength</u>	<u>Mineral Phases</u>
Control (dried at 110°C and fired to 1010°C)	9.6 $\pm$ 2.1 MPa 1,400 $\pm$ 300 psi	Mullite, cristobalite, CaO·Al <sub>2</sub> O <sub>3</sub> , α-alumina [trace: anorthite (triclinic) and CaO·2Al <sub>2</sub> O <sub>3</sub> ]
17 h at 400°C and 2.07 MPa of steam	13.1 $\pm$ 1.5 MPa	Mullite, cristobalite, anorthite (triclinic and only moderately crystallized), α-alumina
100 h at 620°C and 4.14 MPa of steam	1,900 $\pm$ 200 psi	[trace: CaO·Al <sub>2</sub> O <sub>3</sub> ]

Following the successful completion of the *in situ* strength determination on the low-alumina refractory concrete after exposure to elevated pressure steam, another experiment was begun on a high-alumina refractory concrete in steam. The experimental procedure was similar to that of the preceding experiment. This experiment was still in progress at the end of the quarter and results will be reported in the next report. The pressure/temperature exposure conditions are 4.55 MPa (660 psia) of steam pressure at 410°C.

Plans: Depending upon the successful completion of the experiment currently in progress, controlled experimental studies will begin on newly prepared batches of both high and low-alumina refractory concretes with steam as the reactive exposure environment. Initial temperatures of consideration will be 310°C, 610°C, and 1010°C. If possible, additional specimens will be exposed with the specimens for the *in situ* testing, so that strength-after-exposure can be correlated with the strength determined at pressure and temperature.

### 3. Chemical Degradation of Ceramics

#### a. Reactions and Transformations (F. A. Mauer and C. R. Robbins, 565)

Progress: A test bar of uncured calcium aluminate binder was exposed to the simulated gasification environment to more accurately determine temperatures of formation and dissociation of several important phases. Duration of the experiment was 300 hours and 25 x-ray patterns were recorded.

The bar consisted initially of  $CA^*$  and  $\alpha-A$ . As discussed in previous reports, formation of  $CC$  and  $AH$  with increasing temperature was observed by the *in situ* x-ray method. At  $650^\circ C$  and 1000 psig\*\* (140 hours of exposure) the pressure slowly decreased to 710 psig, as a result of partial failure of a gasket in the vessel. The experiment was continued with additions of dry gas mixture (42%  $H_2$ , 33%  $CO$ , 25%  $CO_2$ ) which helped maintain the desired pressure as the steam content of the environment was depleted.

After 300 hours, the experiment was terminated at  $900^\circ C$  and 540 psig. The phases present were  $\alpha-A$ ,  $CC$ , a small amount  $CA_2$  and a trace of  $CA$ . In the presence of steam,  $CC$  dissociates at  $\sim 700^\circ C$  in the simulated environment. In the dry gas mixture it appears to be a stable phase at  $975^\circ C$ .

A bar of  $CC$  was prepared in order to observe the behavior of this compound in more detail. In preliminary experiments, a series of patterns were recorded at  $100^\circ$  intervals from ambient to  $1100^\circ C$  at a constant pressure of  $CO_2$  of 500 psig.  $CC$  has been reported [1] to dissociate at about  $1100^\circ C$  (500 psig  $CO_2$ ). *In situ* x-ray diffraction patterns of the  $CC$  bar of this experiment showed no evidence of dissociation at  $1100^\circ C$  (500 psig). Further work is planned with this compound.

Phase analyses of refractory specimens from a modulus of rupture study were made by conventional x-ray methods for Task 2. Results will be given under that section.

Plans: Test bars of  $CC$  will be studied in several atmospheres. Test bars of  $CAS_2$  will be studied in the simulated gasification atmosphere.

\* $C=CaO$ ;  $A=Al_2O_3$ ;  $H=H_2O$ ;  $CC=CaCO_3$

\*\*In SI units, 1 MPa  $\approx$  14.5 psia.

[1] R. I. Harker and O. F. Tuttle, Amer. Journ. Sci., Vol. 253, p. 209 (1955).



b. Slag Characterization (W. S. Brower, J. L. Waring, and D. H. Blackburn, 565)

Progress: As discussed in previous quarterly reports a synthetic coal slag with the following composition: SiO<sub>2</sub>, 48%; Al<sub>2</sub>O<sub>3</sub>, 12.10%; Fe<sub>2</sub>O<sub>3</sub>, 12.00%; CaO, 14.90%; MgO, 8.00% Na<sub>2</sub>O, 4.7% (expressed in wt percent) has been investigated.

The viscosity of this material was found to decrease significantly in a total nitrogen pressure of 25 psi from  $\log \eta = 1.84$  (value in air) to  $\eta = 1.71$  at 1279°C. Most probably this reduction in the viscosity can be attributed to an increase in the Fe<sup>2+</sup> in the melt as it is well established that oxides containing Fe<sup>3+</sup> will thermally reduce in air at temperatures of 1300 to 1400°C, with the Fe<sub>2</sub>O<sub>3</sub> ↔ Fe<sub>3</sub>O<sub>4</sub> transition occurring at ~1425°C. The reduction of the Fe<sup>3+</sup> ion would be greater in N<sub>2</sub> or steam (P<sub>O<sub>2</sub></sub> ~ 10<sup>-4</sup> - 10<sup>-5</sup> atm). An attempt was made to remelt this material (previously melted under 25 psi N<sub>2</sub> pressure) and crystallization occurred. From our results to date it appears that any heat treatment of a low alkali iron bearing slag in a reducing environment will decrease the viscosity as compared to results obtained in air at the same temperature. It is becoming more obvious as these experiments progress that viscosity is not independent of the previous heat treatment and that once crystallization occurs remelting is very difficult. It would seem then that for a given pressurized process relying on the removal of coal ash via the slag route it is advisable not to operate in the regime where crystallization occurs due to the difficulty in remelting. It might be important to have a thorough knowledge of the effect of additives on the retardation of slag recrystallization caused by inadvertent "cool down".

A considerable number of experiments were made in the pressure range of 50 to 75 psi steam at about 1360°C. Wide scatter in the data appeared to be caused by problems with the temperature control system. To correct the temperature control problem another controller was substituted. Considerable time was spent adjusting the proportional band and reset to obtain adequate control action. The viscosity of the slag was measured while controlling the temperature to ±5°C at 80 psi. The values obtained are given in the following table.

Temperature °C	Viscosity log $\eta$ ambient pressure	Viscosity average log $\eta$ at 80 psi steam
1275	1.88	1.71
1296	1.76	1.65
1351	1.56	1.50
1370	1.44	1.44

The results are shown in figure 1. The viscosity appears to be lowered with increasing pressure. In addition, the value of  $\log \eta = 1.44$  at  $1370^{\circ}\text{C}$  at both ambient pressure and 80 psi steam indicates that the two viscosity curves tend to intersect with increasing temperature, it is conceivable that these two curves could cross, however, our measurements have not been extended high enough in temperature to actually distinguish between the two.

In the next experiment 25 psi of  $\text{CO}_2$  was introduced into the melt. However, a leak developed in the apparatus. When the experiment was redone trouble developed and the power supply was incinerated. Consequently the power supply was returned to the manufacturer for repair which caused several weeks delay.

In the last experiment for the reporting period an attempt was made to determine the viscosity of this material in  $\text{CO}_2$  and steam. Ten psi of  $\text{CO}_2$  was added to 55 psi of steam in the viscometer. Earlier the material was heated briefly in  $\text{CO}_2$  and some crystals had apparently formed on the surface of the melt. When the bob was introduced into the melt it apparently contacted the crystalline mass, moved off center and effectively was welded to the side of the crucible. This ruined the crucible containing the melt and the suspension.

The suspension was rebuilt and a new crucible has been placed in service and the apparatus is again ready to measure viscosity.

Plans: Measure the viscosity of a synthetic slag in  $\text{CO}_2$  and steam and continue the process with other mixed gases and steam.

From the above data a second generation viscometer should be built with higher temperature and pressure capabilities. This problem will be addressed.

	wt %
SiO <sub>2</sub>	48.30
Al <sub>2</sub> O <sub>3</sub>	12.10
Fe <sub>2</sub> O <sub>3</sub>	12.00
CaO	14.90
MgO	8.00
Na <sub>2</sub> O	4.70

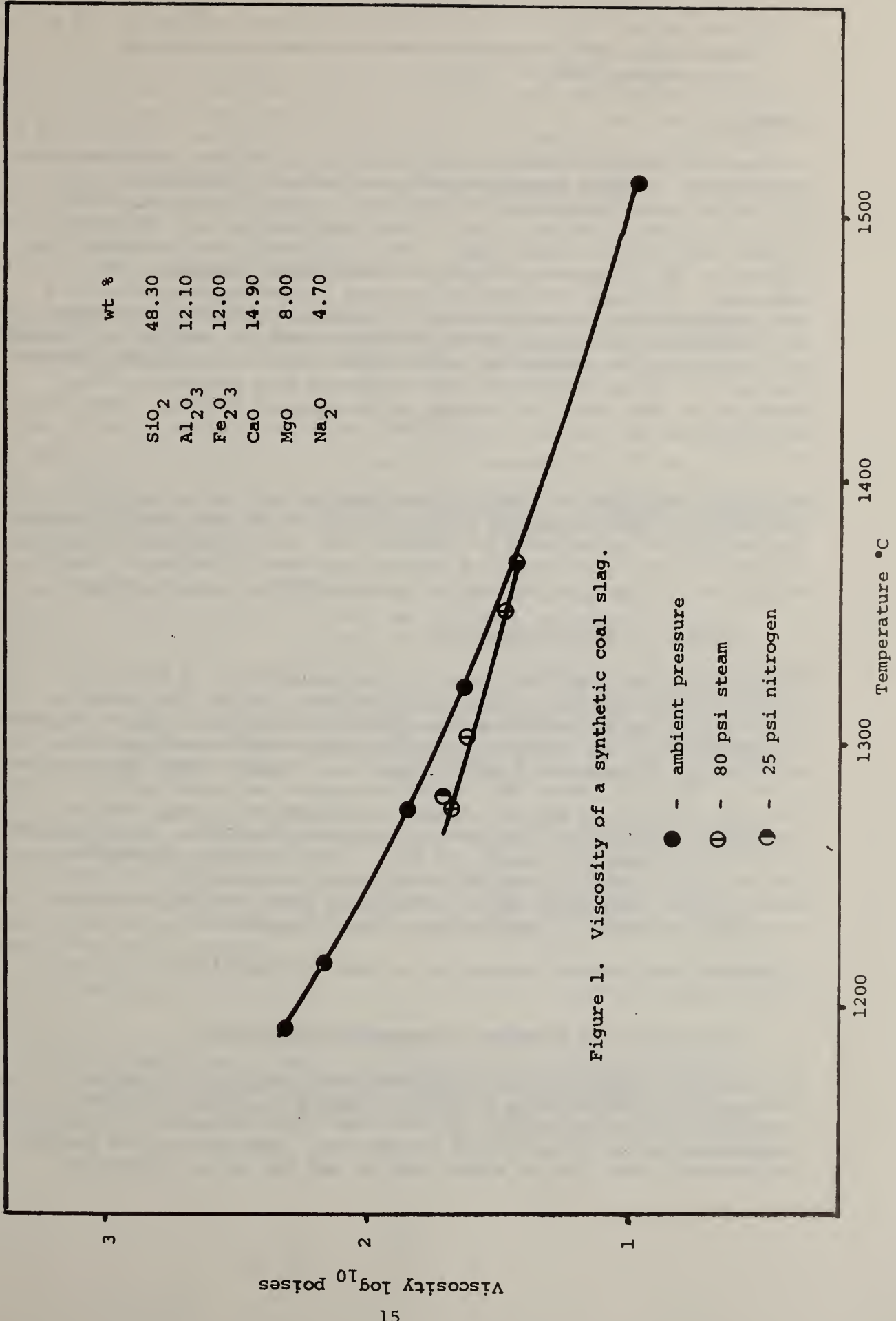


Figure 1. Viscosity of a synthetic coal slag.

- - ambient pressure
- ⊕ - 80 psi steam
- ⊙ - 25 psi nitrogen

- c. Vaporization and Chemical Transport (J. Hastie, D. Bonnell, and E. Plante, 561)

Progress:

An extensive study has been made of vapor transport over a high melting temperature ( $\sim 1700\text{K}$ ) potassium-enriched coal slag (Illinois no. 6). The initial slag composition, in wt%, was:  $\text{Al}_2\text{O}_3$  (12.06),  $\text{CaO}$  (3.8),  $\text{Cr}_2\text{O}_3$  (1.3),  $\text{Fe}_2\text{O}_3$  (14.25),  $\text{K}_2\text{O}$  (19.54),  $\text{MgO}$  (1.03),  $\text{Na}_2\text{O}$  (0.47),  $\text{SO}_3$  (0.21),  $\text{SiO}_2$  (46.82),  $\text{TiO}_2$  (0.52). This slag sample was obtained from combustion of Illinois no. 6 coal with additional potassium added to the combustor. Although this high  $\text{K}_2\text{O}$  content is not representative of a coal gasifier slag it serves a useful purpose in extending the temperature and composition range over which pertinent transport data can be obtained. For identification purposes we shall denote this high potassium content slag as  $\text{K}_1$ . X-ray diffraction data indicated that the bulk of the potassium in the slag  $\text{K}$  is present as the compound  $\text{KAlSiO}_4$ . About 2% of the potassium was present in relatively volatile form, mainly  $\text{K}_2\text{SO}_4$  and  $\text{K}_2\text{CO}_3$ .

We present here data on vapor species identity and vapor transport dependence on temperature,  $\text{N}_2$  carrier gas pressure, and slag  $\text{K}_2\text{O}$  content. The results are interpreted to indicate that the bulk of the potassium is highly bound in the slag and that its release to the vapor phase is controlled, in part, by the rate of alkali diffusion to the surface.

1. Identity of Volatile Species

The potassium-enriched coal slag,  $\text{K}_1$ , was subjected to a series of heating cycles (runs) in nitrogen carrier gas. During the initial heating cycle mass spectral scans, obtained using the transpiration mass spectrometric (TMS) technique, revealed many volatile species, in addition to the expected  $\text{K}$  and  $\text{Na}$  species. A typical mass spectrum is given in figure 1, where the following species can be positively assigned:  $\text{H}_2\text{O}$ ,  $\text{CO}_2$ ,  $\text{SO}_2$ ,  $\text{O}_2$ ,  $\text{K}$  and  $\text{Na}$ . Some of the other ion signals can be tentatively assigned to the species (some hypothetical):  $\text{KO}$  or  $\text{KOH}$ ,  $\text{KS}$  or  $\text{KSH}$ ,  $\text{SiS}$ ,  $\text{SiSH}$ ,  $\text{H}_2\text{S}$ ,  $\text{H}_2\text{SO}_2$  and  $\text{KSiO}$ . From the JANAF thermochemical tables we can expect to see  $\text{KOH}$  under these conditions but not  $\text{H}_2\text{S}$ . Some of these more minor species may result from slag occlusions and would not represent an equilibrium release from the slag.

Following this initial heating cycle, the only significant slag vapor species were  $\text{K}$  and  $\text{O}_2$ .

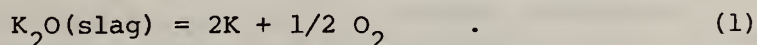
2. Species Partial Pressure - Temperature Dependence

The initial volatiles showed a non-monotonic variation of partial pressure with temperature, as shown in figure 2. These volatiles constitute only a few percent of the total slag components and are not representative of the bulk slag composition. However, they do provide a sufficiently high flux of alkali ( $\text{Na}$ ,  $\text{K}$ ) and  $\text{SO}_2$  to be a potential

source of corrosion. The high initial partial pressures of  $\text{SO}_2$ ,  $\text{CO}_2$ , K and Na are indicative of the presence of alkali sulfate and carbonate in the slag. An additional contribution to low temperature alkali release could result from the high  $\text{H}_2\text{O}$  content leading to the formation of volatile hydroxide species (KOH) at  $T < 1250\text{K}$ . Note that at  $T > 1400\text{K}$  the K pressures fall below those expected from  $\text{KAlO}_2$ , but that the  $\text{SO}_2$ ,  $\text{CO}_2$  and  $\text{H}_2\text{O}$  pressures are still relatively high. Apparently, at this stage, the K produced by sulfate and carbonate decomposition is retained in the bulk slag. After further heating at  $1620\text{K}$  for about 30 min., the sample was virtually depleted of Na,  $\text{SO}_2$  and  $\text{CO}_2$ ;  $\text{H}_2\text{O}$  also continued to fall off in pressure to a negligible level.

### 3. Potassium Partial Pressure-Temperature Dependence

The variation of K-partial pressure was followed over a wide temperature range ( $\sim 1150$ - $1820\text{K}$ ). In general, the  $\text{O}_2$  partial pressure tracked with the K data indicating the main vaporization process to be:



At temperature corresponding to K-partial pressures of  $10^{-5}$  atm, or less, the rate of loss of  $\text{K}_2\text{O}$  from the bulk was sufficiently low that the data represent constant composition conditions. At higher temperatures, and vaporization rates, the data are greatly modified by the effects of changing slag composition.

Typical data are given in figure 3. In order to obtain accurate data at K-partial pressures below  $10^{-5}$  atm, use was made of Knudsen effusion mass spectrometry (KMS). A relatively high background signal at 39 amu (K position) limited the sensitivity of the transpiration mass spectrometric (TMS) measurements. By combining both the TMS and KMS methods we were able to cover a wide range of temperature and  $\text{K}_2\text{O}$  mole fraction conditions. The rate of vapor transport differs appreciably for the two methods, with KMS losing about three times as much material as for TMS. Thus the bulk slag composition changes more rapidly during a KMS experiment.

The  $\text{N}_2$  carrier gas used for the TMS experiments also contained a small, but significant, amount of  $\text{O}_2$  (typically  $\sim 5 \times 10^{-5}$  atm). This should cause a slight suppression of the K-vapor pressure by a reversal of reaction (1). When this effect is taken into account, using the observed thermochemical data for reaction (1), good agreement is found between the TMS and KMS data at the comparison temperature ( $1515\text{K}$ ) and composition point (see fig. 3).

### 4. $\text{K}_2\text{O}$ Activity Coefficients

As most of the bulk-slag composition changes result from reaction (1), a continuous monitoring of the K-partial pressure (and  $\text{O}_2$ ) allows one to calculate the slag composition at any stage of an experiment. For instance, with the TMS method, the number of moles (n) of  $\text{K}_2\text{O}$  lost by

vapor transport (as  $K + O_2$ ) is related to the known mole number and pressure of  $N_2$  by the transpiration relationship:

$$n(K_2O) = \frac{[n(N_2) + n(K_2O)] P_{K_2O}}{P_{N_2}} \quad (2)$$

Hence the change in composition with time can be determined, provided the initial sample weight and composition are known. Likewise, with the KMS method, the Knudsen effusion equation (integrated intensity-time form) may be used to follow the bulk-slag composition. For both the TMS and KMS methods, the basic experimental requirement for monitoring the bulk composition is the measurement of significant species partial pressures as a function of time during an experimental run. An independent check on this approach is provided by gravimetric analysis of the sample remaining at the end of a run. Such an analysis has not yet been performed on the post run slag samples. However, when all significant species are monitored, and their ionization cross sections are known, the in situ approach provides a good mass balance at any stage of the experiment, as was shown for the NaCl test system (see previous Quarterly reports).

Since the mole fraction of  $K_2O$  is defined at any stage of an experiment it is possible to convert K-partial pressures to  $K_2O$  activity coefficients. By varying the amount of  $K_2O$  present in the slag during a vaporization run we were able to follow the dependence of  $K_2O$  "apparent" thermodynamic activity on temperature and composition. The term "apparent" is used to emphasize that the slag system may not be in a complete state of thermodynamic equilibrium.

Typical data, expressed in activity coefficient form, are given in figure 4. Activity coefficients ("apparent") were calculated from the experimental K-partial pressures using the expression:

$$\gamma(K_2O) = \frac{P_K^2 \left(\frac{P_K}{4}\right)^{1/2} [\text{slag}]}{P_K^2 \left(\frac{P_K}{4}\right)^{1/2} [\text{pure } K_2O \text{ reference}] X(K_2O)}$$

where  $X(K_2O)$  is the slag  $K_2O$  mole fraction, determined from the calculated mass loss using the integrated ion intensity-time method. The  $K_2O$  reference state data were obtained from the literature. This expression assumes congruent vaporization according to reaction (1). That this is the appropriate reaction was confirmed by KMS observations of  $O_2$  in the appropriate ratio to K, to a reasonable approximation.

Note in figure 4, the non-monotonic nature of the  $\log \gamma(K_2O)$  vs  $T^{-1}$  curves. For normal non-ideal solution behavior, we would expect a linear monotonic relationship with a negative slope representing a negative partial molar enthalpy of solution for  $K_2O$  in the slag. This type of behavior occurs

for segments of each run (see fig. 4), e.g., for run 1, up to about 1430 K, and for run 2 between 1430 and 1630 K. The run 1 data were obtained during the initial heating period when  $K_2SO_4$  and  $K_2CO_3$  decomposition was a significant source of K. The rapid reduction in  $\gamma(K_2O)$  as the temperature is increased beyond 1430K results from the almost complete depletion of these relatively volatile forms of potassium. For runs 2 and 3, the initial reduction of  $\gamma(K_2O)$  with increasing temperature is believed to be due to diffusion limited (in solid slag) K-transport to the slag surface. The onset of increasing  $\gamma(K_2O)$  with temperature is believed to arise from a physicochemical change in the slag leading to a less viscous form, thereby reducing the diffusion limitation. At higher temperatures the bulk composition changes rapidly (see mole fractions in fig. 4) and leads to a peaking in  $\gamma(K_2O)$ .

These unusual data (fig. 4) clearly indicate the difficulty involved in making a priori predictions of slag vaporization behavior. However, the low  $\gamma(K_2O)$  values clearly indicate the highly bound character of  $K_2O$  in the slag.

#### 5. Effect of $N_2$ -Pressure and Flow Rate on K-Pressure

With the TMS technique, partial pressures should be independent of carrier gas pressure and flow rate, if the system is at thermodynamic equilibrium. However, under low activity conditions, such as those found with the  $K_1$  slag, mass transport limitations are possible. The data of figure 5 demonstrate that this is indeed the case with the present slag system.

At  $N_2$  pressures in excess of 0.35 atm, the gas flow rate is sufficiently high that gas unsaturation occurs. The plateau at 0.25-0.35 atm  $N_2$  suggests saturation for these gas flow conditions. That is, the K at the slag surface is at local thermodynamic equilibrium with the bulk gas stream. This condition does not imply, however, the presence of a thermodynamic equilibrium between the bulk and surface slag K. At pressures below 0.25 atm, the rapid increase in K-pressure with decreasing  $N_2$ -pressure, and flow rate, suggests a competition between the rate of K-diffusion through the slag and the rate of removal from the surface by the carrier gas. Apparently, the diffusion process is too slow with respect to the carrier gas flow to maintain an equilibrium surface concentration of K.

A reasonable upper limit approximation to the equilibrium state can be obtained by extrapolating the curve of figure 5 to zero  $N_2$  gas flow rate. This extrapolation indicates that the equilibrium partial pressure for K is about a factor of ten higher, or less, than the observed values at the normal operating pressure of 0.55 atm  $N_2$ . The KMS data should also be diffusion limited as the rate of surface depletion is even greater than with the TMS method. Thus the true equilibrium values of  $\gamma(K_2O)$  are probably greater, by up to an order of magnitude, than those indicated in figure 4; and similarly for the partial pressure data of figures 1-3. Additional measurements on slags of different viscosity, diffusion, and vaporization rates are needed to further elucidate these flow dependent phenomena.

## Plans

We plan to extend this study to include the effects of variable applied  $H_2O$  pressure and of chloride additions to the release of K from the  $K_1$  slag system. Similar studies will also be initiated on a relatively low melting ( $<1500K$ ) synthetic slag of composition wt%,  $SiO_2$  (47.3),  $Al_2O_3$  (11.1),  $Fe_2O_3$  (12),  $CaO$  (13.9),  $MgO$  (7.0), and  $K_2O$  (8.7). Complementary mathematical modeling of alkali vaporization from these slags, and their equilibrium reactions with coal gas constituents, will also be initiated.



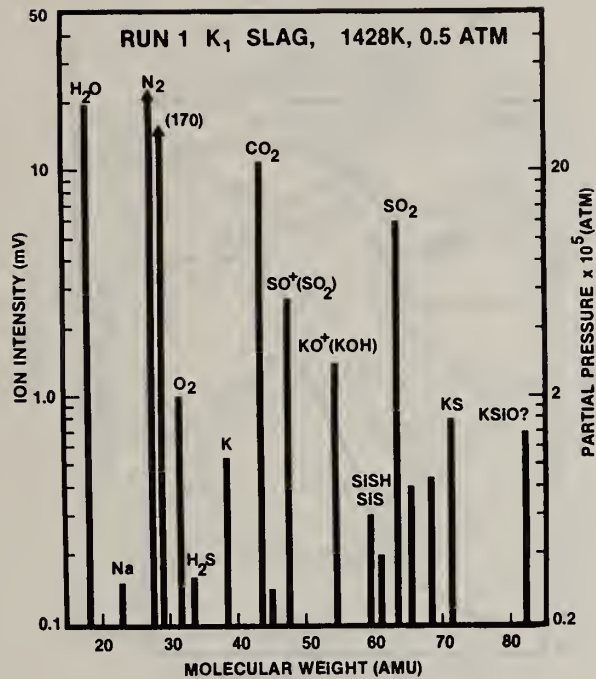


Figure 1. Typical mass spectrum (30eV electron energy) of species evolved from a K-enriched Illinois number 6 coal slag,  $K_1$ , (see text for composition) during an initial heating phase. Data were obtained using the TMS method with a capillary sampling probe. The ordinate (right hand side) indicates approximate partial pressures,  $P_i$ , obtained from  $P_i = k_{N_2} I_i T$ , where  $I_i$  is species  $i$  signal intensity and  $k_{N_2}$  is the instrument sensitivity constant for  $N_2$ ;  $I_{N_2}^{29} = 170$  mV.

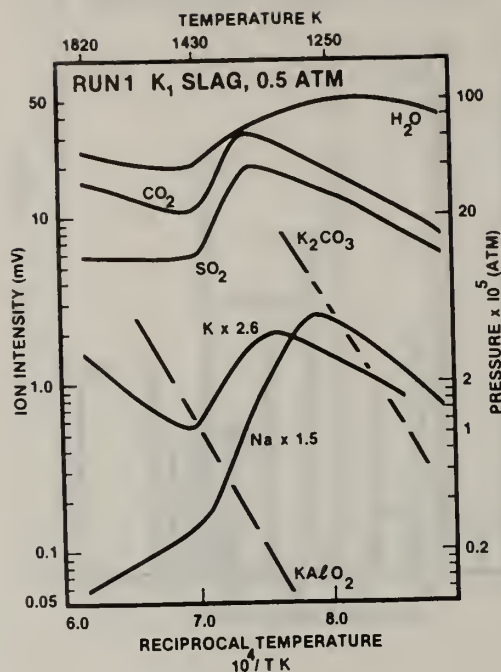


Figure 2. Ion intensity and partial pressure variation of initial volatiles ( $K_2O$  wt% 19.5-19.1) as a function of temperature for the  $K_1$  slag (m.pt.  $\sim 1700 \pm 30K$ ). Pressures,  $P_i$ , were obtained from the ion intensities  $I_i$  using the relation  $P_i = k_i I_i T$ , where  $k_i$  is obtained from  $k_{N_2}$  and the appropriate cross section and sensitivity factors (shown for

$K$  and  $Na$ ). The multiplying factors for  $K$  and  $Na$  refer only to the pressure scale, i.e.  $K \times 2.6 = \text{pressure } K$ ). Literature Clausius Clapeyron curves for  $K$ -pressures from  $K_2CO_3(l)$  and  $KAlO_2(s)$  are also shown for comparison. No literature data are available for  $KAlSiO_4$ , the main  $K$ -containing constituent in this slag, and the  $KAlO_2$  data are considered as an upper limit to the vaporization rate for the silicate.

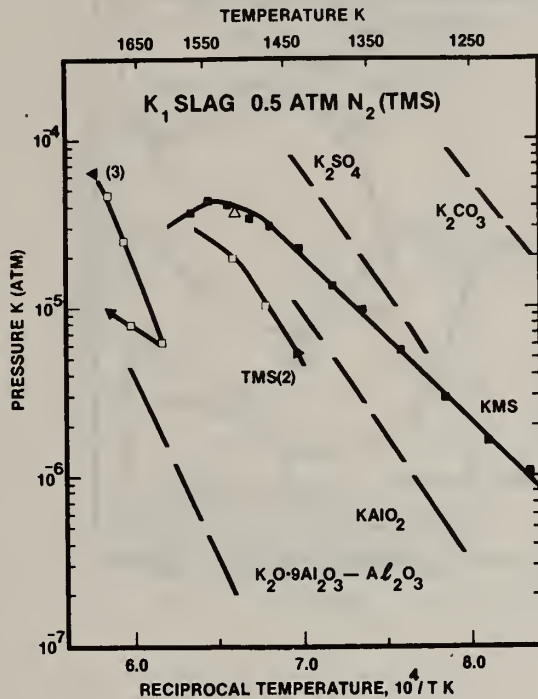


Figure 3. Variation of K-partial pressure with temperature for  $K_2O$  contents of 19.1-17.8 wt% (closed squares, KMS), 18.17-18.07 wt% (run 2- open squares, TMS), and 18.07-18.0 (run 3, open squares, TMS). Corresponding pressure curves (literature data) for the phases  $K_2CO_3(l)$ ,  $K_2SO_4(l)$ ,  $KAlO_2(s)$ , and  $K_2O \cdot 9Al_2O_3 - Al_2O_3 (s)$  are given for comparison. The triangular point at 1515 K is a TMS data point corrected for the presence of  $O_2$  (see main text). Each curve represents a separate experimental run. Usually, data were obtained for successive increases in temperature except for run 3--TMS where the arrows indicate the run chronology, i.e. T increasing or decreasing.

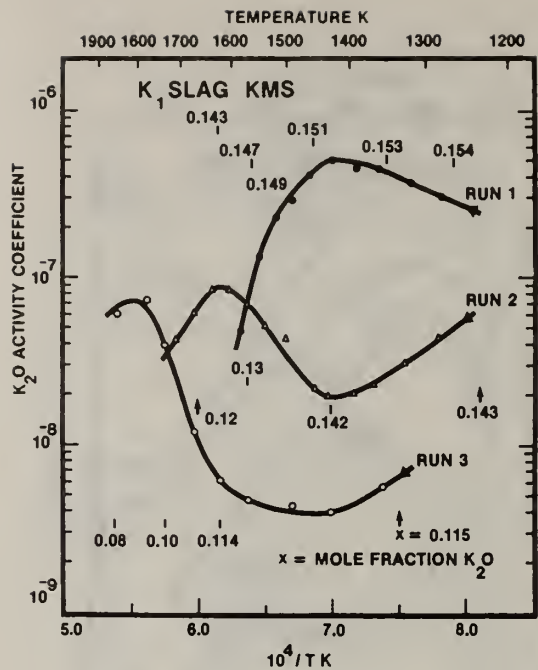


Figure 4. Variation of K<sub>2</sub>O activity coefficient,  $\gamma(K_2O)$ , with temperature and composition for the K<sub>1</sub> slag. The numbers, ranging from 0.154 to 0.08, refer to the mole fraction of K<sub>2</sub>O remaining in the sample at each measurement point. Runs 1-3 were carried out consecutively on the same sample.

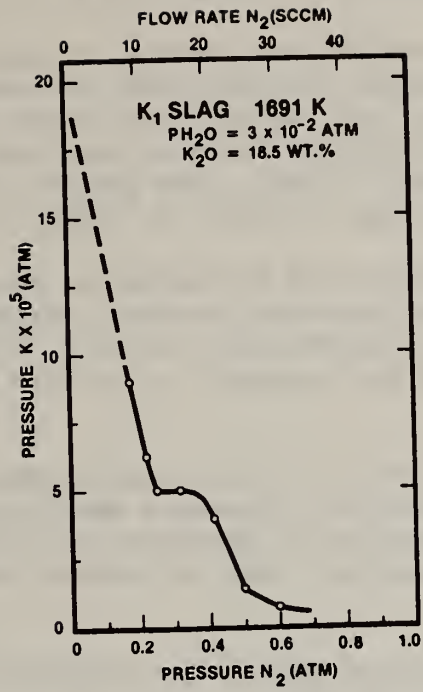


Figure 5. Effect of N<sub>2</sub>-pressure and flow rate on apparent K-pressure at T = 1691±3K and P<sub>H<sub>2</sub>O</sub> = 3 x 10<sup>-2</sup> atm.

#### 4. Failure Prevention

##### a. Failure Information Center (R. C. Dobbyn and W. A. Willard, 562)

Progress: During the quarter the Failure Information Center received eight reports of operational experiences and materials and components failures in coal conversion pilot plants and process development units. This number includes several diagnostic failure analyses from the Argonne and Oak Ridge National Laboratories. To date, the percent contribution of information items contained in the data base is shown in Table 1.

These reports have been classified and evaluated for technical completeness and accuracy and discrepancies have been resolved. Detailed abstracts of this information have been entered into the Center's computerized data bank. A recent update of the frequency of failure modes is shown in Table 2.

The **Information** Center continued to aid Battelle-Columbus in their preparation of the DoE Materials and Components Newslettter feature on failure experiences. Weekly updates of abstracts are furnished to Battelle, together with complete hard copy of certain reports when requested.

The Information Center also handled eight other requests for information during the quarter. In response to these inquires, copies of 343 abstracts and 43 hard copy reports were transmitted.

During this quarter, the review of the report addressing materials performance at the Conoco Lignite Gasification Pilot Plant was completed. Outside reviewers comments have been incorporated into a final draft, additional figures have been prepared and the report has entered the NBS editorial review process.

Progress was also made in further analyzing reported corrosion and erosion failures. The analysis of the data base holdings on corrosion failures was completed during the quarter and a draft report is in preparation. Further analysis of erosive wear failures indicated that 54% of pump failures and 43% of reported valve failures are attributable to erosion; the average incidence of erosion as a principal failure mode is approximately 20-23%. This study will continue.

Work also continued on transferring the Failure Information data base to the new system which will combine this base with the materials properties data base. In addition, the Failure Information Center has begun work with the Materials Properties Data Center on a Performance and Properties Handbook of Construction Materials for Coal Gasification (see section 4b).

Liason with pilot plants and failure analysis laboratories continued. Project staff visited Oak Ridge National Laboratory and planned visits to coal liquefaction plants are being coordinated with the Oak Ridge failure analysis team.

Plans: Plans for the next quarter include: completing the draft report on a detailed analysis of corrosion failures, completion of one section of the Performance and Properties handbook, visits to SRC Wilsonville, SRC Ft. Lewis and the Exxon process development plant near Baytown, Texas.

Table 1

## COAL CONVERSION PROCESSES

NO. OF ITEMS	PERCENT	PROCESS
17	3.49	BIGAS
37	7.61	BMI
7	1.44	CARBONATE
15	3.08	CLEAN COKE
1	0.20	COED
52	10.69	CO2
2	0.41	CPC
21	4.32	CRESAP
2	0.41	EXXON
3	0.61	GFERC
64	13.16	HYGAS
1	0.20	LERC
10	2.05	LIGNITE
19	3.90	MERC
24	4.93	MISC.
2	0.41	PERC
22	4.52	SRC
7	1.44	SRC-W
145	29.83	SYNTHANE
4	0.82	SYNTHOIL
31	6.37	WESTINGHOUSE

486 = TOTAL NUMBER OF ITEMS IN FILE



Table 2

NUMBER OF REPORTED INCIDENTS OF FAILURES  
IN COAL CONVERSION PLANTS \*, \*\*

FAILURE MODE ANALYSIS

FAILURE MODE	PROCESS					TOTAL
	CO2	HYGAS	SRC	SYNTHANE	OTHER	
CORROSION	36	31	8	34	55	164
AQUEOUS	0	1	0	0	3	4
CARBURIZATION	8	1	0	0	3	12
METAL DUSTING	4	0	0	0	3	7
OXIDATION	2	4	0	0	5	11
PITTING	2	4	3	10	9	28
SULFIDATION	13	12	0	6	5	36
GENERAL	7	9	5	18	27	66
STRESS-CORROSION	4	5	5	7	26	47
CHLORIDE	3	5	2	5	8	23
OTHER	1	0	3	2	18	24
MANUFACTURING DEFECT	11	7	8	35	52	113
DESIGN	5	4	8	21	39	77
FABRICATION	3	2	0	5	3	13
QUALITY CONTROL	3	1	0	9	10	23
EQUIPMENT MALFUNCTION	5	11	2	8	20	46
OVERHEAT	5	9	2	6	16	38
OVERSTRESS	0	2	0	2	4	8
EROSION	7	13	6	33	45	104
STRESS/TEMP. FAILURE	1	6	0	6	17	30
CREEP	0	1	0	0	3	4
FATIGUE	0	2	0	3	10	15
THERMAL STRESS/SHOCK	1	3	0	3	4	11
UNKNOWN	3	10	0	30	15	58

\*INCIDENTS REPORTED TO NBS FAILURE INFORMATION CENTER SPONSORED BY DOE-FOSSIL ENERGY

\*\*OPERATING TIMES AND LEVEL OF REPORTING VARY WITH EACH PLANT

- b. Materials Properties Data Center (H. M. Ondik, T. A. Hahn, and  
A. Perloff, 565, and I. J. Feinberg,  
562)

Progress: The handling, cataloging, and filing of reports of materials research projects in Fossil Energy Coal Conversion and Use and for MHD Power Generation continue as regular operations of the Data Center.

At the request of the DOE project monitor we have prepared and submitted under separate cover an outline for a Handbook of data for materials of construction for coal gasification use. The outline, the result of the combined effort of the staff of the Failure Information Center and the Materials Properties Data Center, has been generally approved by the project monitor. The Handbook will aim to provide a ready reference for available information about construction materials of importance for coal gasification processes. There will be four major sections in the Handbook as presently planned. (It is understood that revisions to the outline described here may occur as the work progresses.)

The first section, Section A, will be entitled "Construction Considerations and Performance Data." The information will be organized according to the major functional areas of gasification plants and the components in these areas. The major headings in Section A will be as follows.

1. Coal Handling and Preparation Equipment
  - 1.1 Conveying Equipment
  - 1.2 Grinding and Crushing Equipment
  - 1.3 Drying Equipment
  - 1.4 Fines Control Equipment
2. Pretreatment Equipment
  - 2.1 Heating Equipment
  - 2.2 Devolatilization Equipment
3. Gasification Reactors
  - 3.1 Vessels
    - 3.1.1 Low-Pressure Processes
    - 3.1.2 Medium-Pressure Processes
    - 3.1.3 High-Pressure Processes
  - 3.2 Refractory Linings and Components
    - 3.2.1 Dry-Bottom Vessels
    - 3.2.2 Slagging Vessels
  - 3.3 Metal Internal Components
4. Gas Clean Up Equipment
  - 4.1 Solids Separation Equipment (Scrubbers, Cyclones)
  - 4.2 Cooling Systems (Quench Systems, Heat Exchangers)
  - 4.3 Gas Removal Systems (Carbon Dioxide, Sulfur Compounds, Nitrogen)

5. Water-Gas Shift Equipment
6. Methanation Equipment
7. Compressors
8. Lockhoppers
9. Piping
  - 9.1 Gas Lines
  - 9.2 Solids Transfer Lines
  - 9.3 Slurry Lines
10. Pumps
  - 10.1 Gas Pumps
  - 10.2 Liquids Pumps
  - 10.3 Slurry Pumps
11. Valves
  - 11.1 Gas Valves
  - 11.2 Liquids Valves
  - 11.3 Slurry Valves
  - 11.4 Solids Valves

There will, in general, be three subsections for each of the above headings and subheadings. The first of these subsections will be named "Operating Requirements" and will be devoted to a brief discussion outlining the materials performance requirements for that portion of the plant. The second section, "Performance Data," will deal with the results of laboratory tests of materials for coal gasification conditions, and also with the results of actual plant experience as such data are available. The major sources of these two categories of information will be the data in the Failure Information Center and the Materials Properties Data Center. The third of the subsections, "Candidate Materials," will be a brief discussion of the data presented, indicating the materials which showed satisfactory performance and which therefore can be designated as candidate materials of construction. Although test and performance information for a large variety of materials will be included in Section A, only those designated as candidate materials will be included in the next section of the Handbook.

The second major division, Section B, entitled "Properties of Candidate Materials," will be subdivided as follows: 1. Alloys, 2. Refractories, 3. Coating and Surface Treatment of Metals. The Alloys subsection will include, for each candidate alloy, the various alloy designations, compositions, general applicability, fabrication characteristics, and properties such as melting range, specific heat, thermal expansion and conductivity, emissivity, microstructure, phase and chemical stability, stress-strain data, hardness, fatigue properties, creep and stress-rupture data, etc. The Refractories subsection will be ordered according to the form (castable, brick, etc.), ASTM performance group and generic designation, identified with brand names as available, and mixing and curing characteristics will be given. The properties will

include density, porosity and pore size, permeability, phase and chemical stability, erosion and abrasion resistance, strength and fracture properties, spalling and cracking behavior, specific heat, thermal expansion and conductivity, etc. The data for coatings will be divided into sections on "Metallic Coatings on Metal Bases" and "Ceramic Coatings on Metal Bases" and the properties included will be much the same as in the preceding properties sections.

Sections A and B will attempt to present the information as completely, and yet as concisely, as possible, in order to be responsive to the needs of plant designers, operators, and others of the coal gasification community. The third section, Section C, "Properties of Experimental Materials" will deal with properties of materials under current development and investigation by DOE research contractors. Although such materials are not commercially available and the data may be sparse, the information should help indicate areas for possible improvement of commercially available materials and also areas in which further research may be beneficial. The fourth section, D, will include the references from which the information has been taken for the Handbook. It is expected that to complete the list of useful information for the various sections of the Handbook that a search of the open literature plus manufacturers' specifications will be necessary.

Work on the Handbook is moving forward. The staff of the Failure Information Center and the Materials Properties Data Center have outlined areas of responsibility for portions of the Handbook and information is being prepared. The first efforts naturally are being concentrated on data for Section A. Construction Considerations and Performance Data, and a portion will be sent early in the next quarter for approval by DOE as to style and content.

The request for bids to obtain computer vendors' services was released by the Department of Commerce in January and is in the hands of various vendors. Replies were to be received originally by a February 27 deadline but this deadline had to be extended. Vendors raised questions about the specifications and extra time had to be granted to allow for their consideration of the Department's responses to the questions. Because of some delays within the Department of Commerce it is expected that the vendors' responses and proposals will not be received until the middle of April. As soon as the bids are received, a review and evaluation of the proposals must be a concentrated effort of the Data Center staff for the few weeks following notification by the Department of receipt of the proposals.

Preparation of information for computer storage continues with tape cassettes being prepared for loading into computer storage as soon as a computer vendor's services are procured.

Planning for a State-of-the-Art Review of MHD materials requirements, requested by the DOE project monitor, is also underway. An outline of the review will be delivered during the next quarter.

Plans: Routine operations of the Data Center will continue. During the next quarter a choice of computer vendor should be completed and arrangements made for the services; a section of the Handbook for coal gasification materials will be delivered, as well as an outline of the State-of-the-Art Review of the current MHD materials situation.

